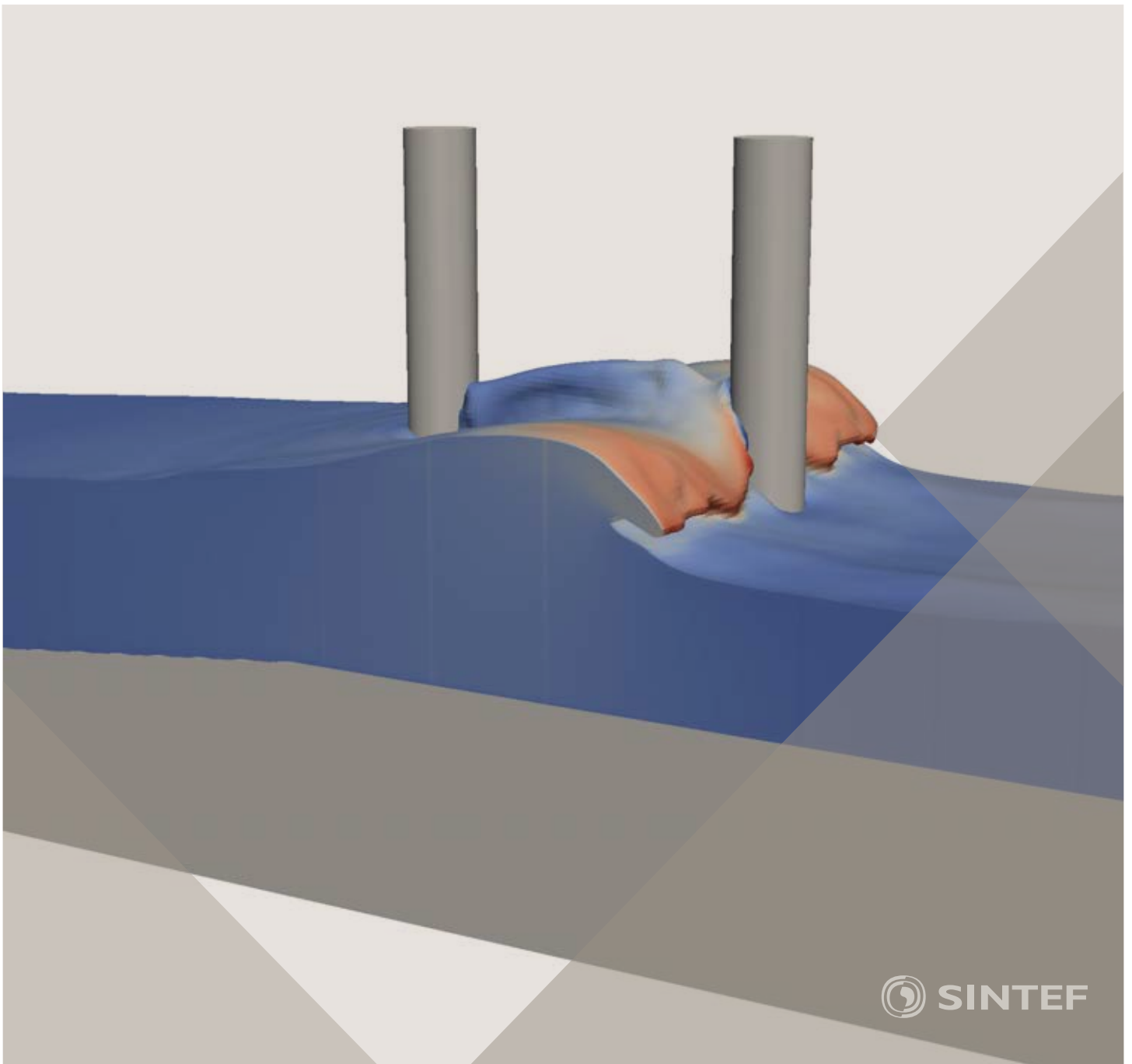


Proceedings of the 12<sup>th</sup> International Conference on  
Computational Fluid Dynamics in the Oil & Gas,  
Metallurgical and Process Industries

# Progress in Applied CFD – CFD2017



SINTEF Proceedings

Editors:

Jan Erik Olsen and Stein Tore Johansen

## **Progress in Applied CFD – CFD2017**

Proceedings of the 12<sup>th</sup> International Conference on Computational Fluid Dynamics  
in the Oil & Gas, Metallurgical and Process Industries

SINTEF Academic Press

SINTEF Proceedings no 2

Editors: Jan Erik Olsen and Stein Tore Johansen

**Progress in Applied CFD – CFD2017**

Selected papers from 10<sup>th</sup> International Conference on Computational Fluid Dynamics in the Oil & Gas, Metallurgical and Process Industries

Key words:

CFD, Flow, Modelling

Cover, illustration: Arun Kamath

ISSN 2387-4295 (online)

ISBN 978-82-536-1544-8 (pdf)

© Copyright SINTEF Academic Press 2017

The material in this publication is covered by the provisions of the Norwegian Copyright Act. Without any special agreement with SINTEF Academic Press, any copying and making available of the material is only allowed to the extent that this is permitted by law or allowed through an agreement with Kopinor, the Reproduction Rights Organisation for Norway. Any use contrary to legislation or an agreement may lead to a liability for damages and confiscation, and may be punished by fines or imprisonment

SINTEF Academic Press

Address:       Forskningsveien 3 B  
                  PO Box 124 Blindern  
                  N-0314 OSLO

Tel:             +47 73 59 30 00

Fax:            +47 22 96 55 08

[www.sintef.no/byggforsk](http://www.sintef.no/byggforsk)

[www.sintefbok.no](http://www.sintefbok.no)

**SINTEF Proceedings**

SINTEF Proceedings is a serial publication for peer-reviewed conference proceedings on a variety of scientific topics.

The processes of peer-reviewing of papers published in SINTEF Proceedings are administered by the conference organizers and proceedings editors. Detailed procedures will vary according to custom and practice in each scientific community.

## PREFACE

This book contains all manuscripts approved by the reviewers and the organizing committee of the 12th International Conference on Computational Fluid Dynamics in the Oil & Gas, Metallurgical and Process Industries. The conference was hosted by SINTEF in Trondheim in May/June 2017 and is also known as CFD2017 for short. The conference series was initiated by CSIRO and Phil Schwarz in 1997. So far the conference has been alternating between CSIRO in Melbourne and SINTEF in Trondheim. The conferences focuses on the application of CFD in the oil and gas industries, metal production, mineral processing, power generation, chemicals and other process industries. In addition pragmatic modelling concepts and bio-mechanical applications have become an important part of the conference. The papers in this book demonstrate the current progress in applied CFD.

The conference papers undergo a review process involving two experts. Only papers accepted by the reviewers are included in the proceedings. 108 contributions were presented at the conference together with six keynote presentations. A majority of these contributions are presented by their manuscript in this collection (a few were granted to present without an accompanying manuscript).

The organizing committee would like to thank everyone who has helped with review of manuscripts, all those who helped to promote the conference and all authors who have submitted scientific contributions. We are also grateful for the support from the conference sponsors: ANSYS, SFI Metal Production and NanoSim.

Stein Tore Johansen & Jan Erik Olsen



Organizing committee:

Conference chairman: Prof. Stein Tore Johansen

Conference coordinator: Dr. Jan Erik Olsen

Dr. Bernhard Müller

Dr. Sigrid Karstad Dahl

Dr. Shahriar Amini

Dr. Ernst Meese

Dr. Josip Zoric

Dr. Jannike Solsvik

Dr. Peter Witt

Scientific committee:

Stein Tore Johansen, SINTEF/NTNU

Bernhard Müller, NTNU

Phil Schwarz, CSIRO

Akio Tomiyama, Kobe University

Hans Kuipers, Eindhoven University of Technology

Jinghai Li, Chinese Academy of Science

Markus Braun, Ansys

Simon Lo, CD-adapco

Patrick Segers, Universiteit Gent

Jiyuan Tu, RMIT

Jos Derksen, University of Aberdeen

Dmitry Eskin, Schlumberger-Doll Research

Pär Jönsson, KTH

Stefan Pirker, Johannes Kepler University

Josip Zoric, SINTEF

## CONTENTS

<b>PRAGMATIC MODELLING .....</b>	<b>9</b>
On pragmatism in industrial modeling. Part III: Application to operational drilling .....	11
CFD modeling of dynamic emulsion stability .....	23
Modelling of interaction between turbines and terrain wakes using pragmatic approach .....	29
<b>FLUIDIZED BED .....</b>	<b>37</b>
Simulation of chemical looping combustion process in a double looping fluidized bed reactor with cu-based oxygen carriers.....	39
Extremely fast simulations of heat transfer in fluidized beds.....	47
Mass transfer phenomena in fluidized beds with horizontally immersed membranes .....	53
A Two-Fluid model study of hydrogen production via water gas shift in fluidized bed membrane reactors .....	63
Effect of lift force on dense gas-fluidized beds of non-spherical particles .....	71
Experimental and numerical investigation of a bubbling dense gas-solid fluidized bed .....	81
Direct numerical simulation of the effective drag in gas-liquid-solid systems .....	89
A Lagrangian-Eulerian hybrid model for the simulation of direct reduction of iron ore in fluidized beds.....	97
High temperature fluidization - influence of inter-particle forces on fluidization behavior .....	107
Verification of filtered two fluid models for reactive gas-solid flows .....	115
<b>BIOMECHANICS.....</b>	<b>123</b>
A computational framework involving CFD and data mining tools for analyzing disease in carotid artery .....	125
Investigating the numerical parameter space for a stenosed patient-specific internal carotid artery model.....	133
Velocity profiles in a 2D model of the left ventricular outflow tract, pathological case study using PIV and CFD modeling.....	139
Oscillatory flow and mass transport in a coronary artery.....	147
Patient specific numerical simulation of flow in the human upper airways for assessing the effect of nasal surgery.....	153
CFD simulations of turbulent flow in the human upper airways .....	163
<b>OIL &amp; GAS APPLICATIONS .....</b>	<b>169</b>
Estimation of flow rates and parameters in two-phase stratified and slug flow by an ensemble Kalman filter .....	171
Direct numerical simulation of proppant transport in a narrow channel for hydraulic fracturing application .....	179
Multiphase direct numerical simulations (DNS) of oil-water flows through homogeneous porous rocks .....	185
CFD erosion modelling of blind tees .....	191
Shape factors inclusion in a one-dimensional, transient two-fluid model for stratified and slug flow simulations in pipes .....	201
Gas-liquid two-phase flow behavior in terrain-inclined pipelines for wet natural gas transportation .....	207

<b>NUMERICS, METHODS &amp; CODE DEVELOPMENT .....</b>	<b>213</b>
Innovative computing for industrially-relevant multiphase flows .....	215
Development of GPU parallel multiphase flow solver for turbulent slurry flows in cyclone.....	223
Immersed boundary method for the compressible Navier–Stokes equations using high order summation-by-parts difference operators .....	233
Direct numerical simulation of coupled heat and mass transfer in fluid-solid systems .....	243
A simulation concept for generic simulation of multi-material flow, using staggered Cartesian grids.....	253
A cartesian cut-cell method, based on formal volume averaging of mass, momentum equations.....	265
SOFT: a framework for semantic interoperability of scientific software .....	273
<b>POPULATION BALANCE .....</b>	<b>279</b>
Combined multifluid-population balance method for polydisperse multiphase flows .....	281
A multifluid-PBE model for a slurry bubble column with bubble size dependent velocity, weight fractions and temperature.....	285
CFD simulation of the droplet size distribution of liquid-liquid emulsions in stirred tank reactors .....	295
Towards a CFD model for boiling flows: validation of QMOM predictions with TOPFLOW experiments .....	301
Numerical simulations of turbulent liquid-liquid dispersions with quadrature-based moment methods.....	309
Simulation of dispersion of immiscible fluids in a turbulent couette flow .....	317
Simulation of gas-liquid flows in separators - a Lagrangian approach.....	325
CFD modelling to predict mass transfer in pulsed sieve plate extraction columns .....	335
<b>BREAKUP &amp; COALESCENCE .....</b>	<b>343</b>
Experimental and numerical study on single droplet breakage in turbulent flow .....	345
Improved collision modelling for liquid metal droplets in a copper slag cleaning process .....	355
Modelling of bubble dynamics in slag during its hot stage engineering.....	365
Controlled coalescence with local front reconstruction method .....	373
<b>BUBBLY FLOWS .....</b>	<b>381</b>
Modelling of fluid dynamics, mass transfer and chemical reaction in bubbly flows .....	383
Stochastic DSMC model for large scale dense bubbly flows.....	391
On the surfacing mechanism of bubble plumes from subsea gas release.....	399
Bubble generated turbulence in two fluid simulation of bubbly flow .....	405
<b>HEAT TRANSFER .....</b>	<b>413</b>
CFD-simulation of boiling in a heated pipe including flow pattern transitions using a multi-field concept .....	415
The pear-shaped fate of an ice melting front .....	423
Flow dynamics studies for flexible operation of continuous casters (flow flex cc).....	431
An Euler-Euler model for gas-liquid flows in a coil wound heat exchanger.....	441
<b>NON-NEWTONIAN FLOWS.....</b>	<b>449</b>
Viscoelastic flow simulations in disordered porous media .....	451
Tire rubber extrudate swell simulation and verification with experiments .....	459
Front-tracking simulations of bubbles rising in non-Newtonian fluids.....	469
A 2D sediment bed morphodynamics model for turbulent, non-Newtonian, particle-loaded flows.....	479

<b>METALLURGICAL APPLICATIONS.....</b>	<b>491</b>
Experimental modelling of metallurgical processes .....	493
State of the art: macroscopic modelling approaches for the description of multiphysics phenomena within the electroslag remelting process .....	499
LES-VOF simulation of turbulent interfacial flow in the continuous casting mold .....	507
CFD-DEM modelling of blast furnace tapping .....	515
Multiphase flow modelling of furnace tapholes .....	521
Numerical predictions of the shape and size of the raceway zone in a blast furnace.....	531
Modelling and measurements in the aluminium industry - Where are the obstacles? .....	541
Modelling of chemical reactions in metallurgical processes.....	549
Using CFD analysis to optimise top submerged lance furnace geometries .....	555
Numerical analysis of the temperature distribution in a martensic stainless steel strip during hardening.....	565
Validation of a rapid slag viscosity measurement by CFD.....	575
Solidification modeling with user defined function in ANSYS Fluent.....	583
Cleaning of polycyclic aromatic hydrocarbons (PAH) obtained from ferroalloys plant.....	587
Granular flow described by fictitious fluids: a suitable methodology for process simulations .....	593
A multiscale numerical approach of the dripping slag in the coke bed zone of a pilot scale Si-Mn furnace.....	599
<b>INDUSTRIAL APPLICATIONS .....</b>	<b>605</b>
Use of CFD as a design tool for a phosphoric acid plant cooling pond .....	607
Numerical evaluation of co-firing solid recovered fuel with petroleum coke in a cement rotary kiln: Influence of fuel moisture .....	613
Experimental and CFD investigation of fractal distributor on a novel plate and frame ion-exchanger .....	621
<b>COMBUSTION .....</b>	<b>631</b>
CFD modeling of a commercial-size circle-draft biomass gasifier.....	633
Numerical study of coal particle gasification up to Reynolds numbers of 1000.....	641
Modelling combustion of pulverized coal and alternative carbon materials in the blast furnace raceway .....	647
Combustion chamber scaling for energy recovery from furnace process gas: waste to value .....	657
<b>PACKED BED.....</b>	<b>665</b>
Comparison of particle-resolved direct numerical simulation and 1D modelling of catalytic reactions in a packed bed .....	667
Numerical investigation of particle types influence on packed bed adsorber behaviour .....	675
CFD based study of dense medium drum separation processes .....	683
A multi-domain 1D particle-reactor model for packed bed reactor applications.....	689
<b>SPECIES TRANSPORT &amp; INTERFACES .....</b>	<b>699</b>
Modelling and numerical simulation of surface active species transport - reaction in welding processes .....	701
Multiscale approach to fully resolved boundary layers using adaptive grids.....	709
Implementation, demonstration and validation of a user-defined wall function for direct precipitation fouling in Ansys Fluent.....	717



<b>FREE SURFACE FLOW &amp; WAVES .....</b>	<b>727</b>
Unresolved CFD-DEM in environmental engineering: submarine slope stability and other applications.....	729
Influence of the upstream cylinder and wave breaking point on the breaking wave forces on the downstream cylinder .....	735
Recent developments for the computation of the necessary submergence of pump intakes with free surfaces .....	743
Parallel multiphase flow software for solving the Navier-Stokes equations .....	752
 <b>PARTICLE METHODS .....</b>	 <b>759</b>
A numerical approach to model aggregate restructuring in shear flow using DEM in Lattice-Boltzmann simulations .....	761
Adaptive coarse-graining for large-scale DEM simulations.....	773
Novel efficient hybrid-DEM collision integration scheme.....	779
Implementing the kinetic theory of granular flows into the Lagrangian dense discrete phase model.....	785
Importance of the different fluid forces on particle dispersion in fluid phase resonance mixers .....	791
Large scale modelling of bubble formation and growth in a supersaturated liquid.....	798
 <b>FUNDAMENTAL FLUID DYNAMICS .....</b>	 <b>807</b>
Flow past a yawed cylinder of finite length using a fictitious domain method .....	809
A numerical evaluation of the effect of the electro-magnetic force on bubble flow in aluminium smelting process.....	819
A DNS study of droplet spreading and penetration on a porous medium.....	825
From linear to nonlinear: Transient growth in confined magnetohydrodynamic flows.....	831

## EXPERIMENTAL MODELLING OF METALLURGICAL PROCESSES

**Gunter Gerbeth\***, Sven Eckert

Helmholtz-Zentrum Dresden – Rossendorf (HZDR), Institute of Fluid Dynamics, 01328 Dresden, GERMANY

\* E-mail: g.gerbeth@hzdr.de

### ABSTRACT

Metallurgical processes often involve multi-phase flows of molten metals or molten slags. No doubt, CFD is a powerful tool to describe such flows, but for complex flow phenomena experimental data are needed for code validation. As for many melts such CFD grade data do not exist, liquid metal model experiments are more and more used in order to fill this gap. Several examples of it are described here.

**Keywords:** Liquid metal model experiments, measurement techniques.

### INTRODUCTION

Metallurgical processes involve a variety of molten metals or molten slags, which are opaque and typically at high temperatures. Measurements in such systems, e.g. of local velocities, temperatures, pressures, void fractions, impurity distributions, etc., are till today very scarce. CFD is a powerful tool in order to develop the necessary process understanding, but without relevant measurement data it is sometimes a bit lost, in particular in case of complex, often turbulent multi-phase processes. A powerful tool to validate related CFD codes consists in slightly simplified, low-temperature liquid metal model experiments. Water model experiments are, instead, often of limited value, particularly in the cases of strong temperature gradients, two-phase flows or flows exposed to electromagnetic fields.

Such liquid metal model experiments became a powerful tool over the past decade, mainly due to the development and availability of measurement techniques allowing to measure, e.g., the flow field in those melts almost completely up to melt temperatures of about 300°C. In the following we present, besides an overview on the measurement techniques, several examples for such kind of liquid metal model experiments. It involves mainly our experimental family LIMMCAST for modelling the continuous casting process of steel.

### MEASUREMENT TECHNIQUES FOR LIQUID METAL FLOWS

Commercial techniques for measuring the flow field in opaque liquids at higher temperatures are only barely available. Substantial research activities have been carried out at HZDR during the last 15 years on the

development and qualification of various methods to measure the velocity field in liquid metal flows. In this connection, we follow a twofold strategy. On one hand, we try to develop measuring techniques for applications under real industrial conditions. On the other hand, we use liquid metal models as an important tool to investigate the flow structure and related transport processes in melt flows being relevant for metallurgical applications. Besides the classical, invasive probes new ultrasonic or electromagnetic techniques came up and allow today a satisfying characterisation of flow quantities in the considered temperature range until 300°C. For reviews of those techniques we refer to Eckert et al. (2007, 2011) and Wondrak et al. (2014).

Today the Ultrasonic Doppler Velocimetry (UDV) and the newly developed Contactless Inductive Flow Tomography (CIFT) are most promising for the measurement of local velocity fields.

The Ultrasound Doppler method was developed in the early 1990's by Takeda (1991) and has been established in science and engineering for fluid flow measurements over the past two decades. UDV gives the one-dimensional velocity profile along the direction of the ultrasonic beam. The use and combination of multiple ultrasonic transducers expands the observation area or extends the number of velocity components which can be measured. The measurement can be done with a direct contact of the transducer to the fluid, but it can operate also through the wall of the liquid metal flow. Commercial transducers are available for temperatures up to about 230°C. For fluids at higher temperatures the concept of using an acoustic wave guide has been developed by Eckert et al. (2003) in order to achieve a thermal as well as a chemical decoupling between the active transducer and the hot fluid. The measurable velocity range extends from about 0.5 mm/s to 3...5 m/s with a spatial resolution of typically 1...5 mm and a temporal resolution of up to 30...50 Hz. The latter means that a full measurement of turbulent spectra is typically not possible with UDV, but the transient behaviour of practically relevant mean flow fields can certainly be monitored.

A new approach for a fully contactless and almost instantaneous detection of mean flow fields in metal melts is available today with CIFT. The melt volume is surrounded by one or two magnetic excitation fields. Magnetic field sensors mounted outside the melt detect

the induced magnetic field which arises from the interaction between the applied field and the flow. These flow-induced magnetic fields allow for a reconstruction of the three-dimensional mean velocity field in the melt as first demonstrated by Stefani et al. (2004). Successful applications of CIFT at single and two-phase flows typical for the continuous casting process have been reported by Wondrak et al. (2010, 2011). The main practical problem for CIFT typically consists in the low values of the flow-induced magnetic fields, which for an applied field of 1 mT are in the order of several ten's or hundred's of nT. This is often a challenging task due to disturbing electromagnetic fields (heaters, valves, pumps, etc.) which usually belong to the set-up at which CIFT shall be applied. Several solutions for an increased robustness of CIFT have recently been developed (AC field excitation, gradiometric pickup coils, improved reconstruction algorithms). Ratajczak et al. (2016) demonstrated that CIFT can operate reliably even in the presence of a strong external magnetic field such as an Electromagnetic Brake (EMBr) at a steel casting model. CIFT delivers mean three-dimensional flow fields with a temporal resolution of about 1 Hz. Measurements in the range of about 10 mm/s up to 5 m/s have been reported.

## LIMMCAST FACILITIES

For the modelling of flow problems in the continuous casting of metals meanwhile three different LIMMCAST facilities have been installed at HZDR. The LIMMCAST programme aims to model the essential features of the flow field in a continuous casting process, namely the flow field in the tundish, in the submerged entry nozzle (SEN) and in the mould as well as the solidification of the material in the strand. Figure 1 shows a photograph of the main, large LIMMCAST facility. All components are made from stainless steel. The low melting point alloy Sn60Bi40 is used as model liquid, whose temperature-dependent material data are well-known (Plevachuk et al., 2010). The liquidus temperature of 170°C allows for an operation of the facility in a temperature range between 200 and 400°C. The melt inventory is stored in two vessels with a capacity of 250 l each. An electromagnetic pump is used to transport the liquid metal into the tundish. The maximum flow rate, which is measured by an electromagnetic flow meter, is about 2.5 l/s.

Figure 2 shows a photograph of the test section containing the tundish, the SEN and the mould. From the tundish the melt pours through a pipe with an inner diameter of 54,5 mm into the mould with a rectangular cross section of 400 × 100 mm<sup>2</sup>. Argon gas bubbles can be injected with tuneable flow rates through the stopper rod into the SEN resulting in a two-phase flow inside the nozzle and the mould. Pipe connections with flanges are realized at various locations within the loop allowing a replacement of the particular components. This regards especially the nozzle, the mould, the tundish and parts of diverse test sections, which gives us a broad flexibility to modify the flow geometries for upcoming requirements.

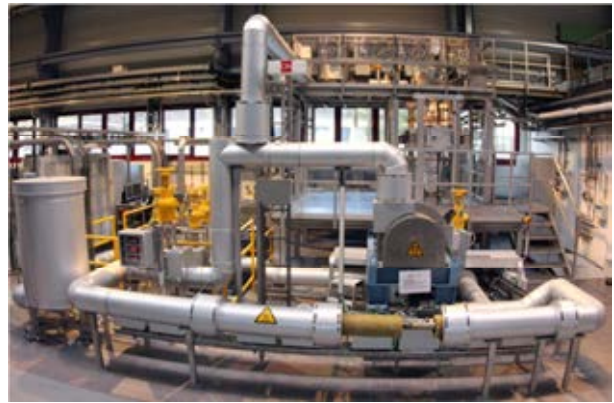


Figure 1: Overall view of the LIMMCAST facility.

A main goal of the research at LIMMCAST consists in investigations on the impact of various types of magnetic fields on the flow in the mould and in the SEN. For instance, an EMBr with rectangular pole faces of 450 × 200 mm<sup>2</sup> has been used where a maximum electrical current of 2000 A provides a magnetic field strength up to 0.7 T within the pole gap of 200 mm. The flexible pole shoe design allows for the investigation of different magnetic field configurations, such as local brakes, ruler or even double ruler brakes.

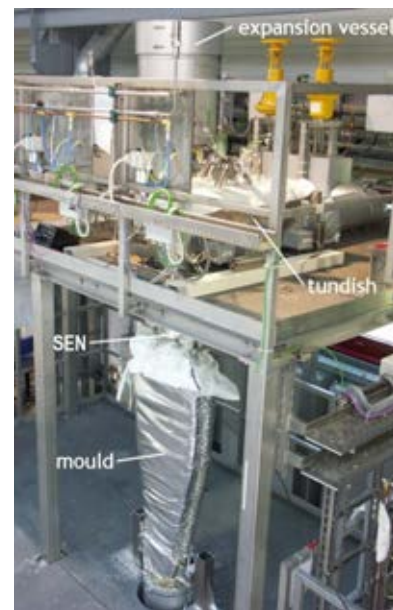


Figure 2: Photograph of the main test section with tundish, SEN and mould.

In addition to the main LIMMCAST facility the two smaller facilities Mini-LIMMCAST and X-LIMMCAST have been built up. Mini-LIMMCAST as shown in Fig. 3 uses the eutectic alloy Ga<sub>68</sub>In<sub>20</sub>Sn<sub>12</sub> as model fluid, which is liquid at room temperature. In contrast to the large LIMMCAST no heating is necessary and experiments can be performed either in a continuous or in a discontinuous way.

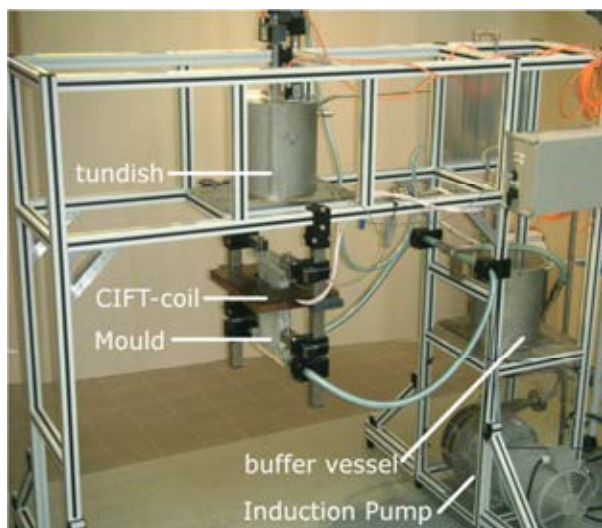


Figure 3: Photo of Mini-LIMMCAST.

The mould with a cross-section of  $140 \times 35 \text{ mm}^2$  and the nozzle with an inner diameter of 10 mm are made of acrylic glass. Stainless steel cylinders work as tundish and buffer vessel, respectively. In the discontinuous mode the tundish was filled with the alloy and then, after the lift of the stopper rod, the liquid metal pours through the nozzle into the mould. The total charge of about 6 litres of the alloy enables a measuring time of about 40 seconds with a mean flow rate of 100 ml/s. A detailed description of LIMMCAST and Mini-LIMMCAST is given by Timmel et al. (2010).

As model of an EMBr a DC magnet is utilized to supply a transverse magnetic field with a maximum field strength of  $B = 310 \text{ mT}$ . The pole faces of the magnet covered the wide side of the mould completely. We considered both situations of an electrically isolated and an electrically conducting mould, respectively. To simulate the case of the solidified shell in the real casting process, which actually exhibits a higher electrical conductivity as the liquid steel, the inner walls of the wide mould face were covered by brass plates with a thickness of 0.5 mm.

The **X-LIMMCAST** facility is a liquid metal loop constructed for use in the X-ray laboratory at HZDR. It is also operated with the model fluid GaInSn at room temperature. Visualisations of the liquid metal – argon two phase flows can be obtained by means of X-ray radioscopy. Figure 4 shows the experimental facility in the HZDR X-ray lab.

The melt is discharged through an acrylic glass tube with an inner square cross section of  $12 \times 12 \text{ mm}^2$  into the mould. The mould was also made from acrylic glass with a rectangular horizontal cross section of  $100 \times 15 \text{ mm}^2$  and a total length from the top lid to the bottom outlet of 426 mm. The liquid metal is circulated by an electromagnetic pump equipped with rotating permanent magnets. A maximum liquid metal flow rate of about 150 ml/s was achieved in the experiments if the stopper rod was brought into the highest position. During the two-phase flow experiments argon gas was injected at the tip of the stopper rod. Gas flow rates were adjusted in a wide range between 50 and 500  $\text{cm}^3/\text{min}$  by means of a mass flow controller. A more

detailed description of X-LIMMCAST and related results are given by Timmel et al. (2015).



Figure 4: Photo of X-LIMMCAST in the X-ray lab of HZDR.

## RESULTS OF THE LIMMCAST MODELS AND RELATED CFD RESULTS

There is meanwhile a vast of experimental and numerical results obtained with respect to the measurements at the LIMMCAST facilities. Here we point out a particular aspect which is interesting with respect to the relation between numerical and experimental modelling. The action of an EMBr was for many years considered as being almost fully understood in the sense that an external steady magnetic field always has a stabilizing influence on the flow of a liquid metal. The DC field was supposed to brake the mean flow and to reduce turbulent fluctuations in all configurations. Indeed, a vast of numerical simulations in the literature clearly showed this behaviour. Timmel et al. (2011) performed systematic studies of the mould flow at Mini-LIMMCAST with and without an external EMBr. Surprisingly it was found that the measured melt velocities showed the tendency of enhanced turbulent fluctuations for increasing magnetic field strength, in particular for the case of an electrically isolating mould wall. Figure 5 shows typical UDV velocity measurements at one fixed position in the core of the jet discharging from a port of the SEN. It clearly demonstrates that the velocity fluctuations in case of the electrically non-conducting mould are enhanced, whereas in case of a conducting mould wall the fluctuations are almost in the same range as without the EMBr. Figure 6 illustrates this behaviour with UDV velocity measurements of higher temporal resolution. Obviously, the steady magnetic field, i.e. the EMBr, triggers low-frequency velocity oscillations.

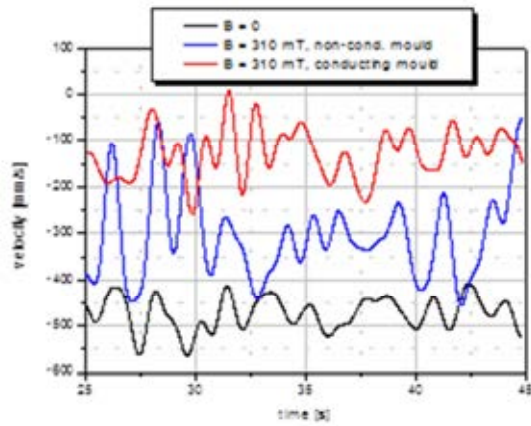


Figure 5: Measured velocities at a fixed position in the core of the jet.

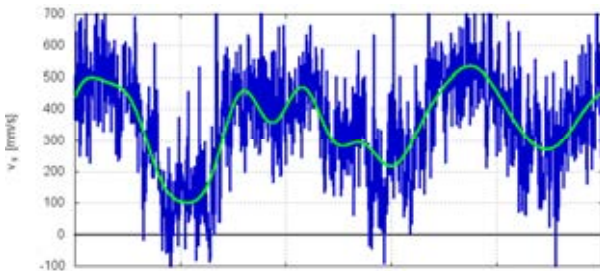


Figure 6: Measured velocity at a fixed position in the mould for electrically non-conducting mould walls.

Most interestingly, shortly after these experimental findings and the additional provision of detailed measurement data, refined numerical simulations by Chaudhary et al. (2012) and Miao et al. (2012) confirmed the results, in particular the tendency that the EMBr may enhance low-frequency oscillations in the velocity field.

There is no physical reason that the effect of a DC magnetic field on a liquid metal flow should only consist in a braking and turbulence damping action, in particular for fully three-dimensional flows. The magnetic field action is essentially determined by the closure of the electrical current, which geometrically results in local non-braking Lorentz forces, in particular for electrically non-conducting walls. Note that there is the case of the magnetorotational instability, which is a rotating flow which shows a laminar-turbulent transition solely due to an increasing external DC magnetic field (Stefani et al., 2006).

For a correct numerical simulation of the mould flow with EMBr two aspects turned out to be crucial:

- sufficient grid resolution of the typical electromagnetic Hartmann layers,
- anisotropic magnetic field effect in the turbulence modelling.

For more details we refer to Miao et al. (2012).

Regarding the two-phase flow in the nozzle and in the mould, the model experiments reported by Timmel et al. (2015) revealed that the gas bubble injection through the stopper rod results in the occurrence of rather large gas cavities in the upper, low-pressure region of the SEN as shown in Fig. 7.



Figure 7: Gas distribution in the upper part of the SEN. Experiments at X-LIMMCAST with a liquid flow rate of  $140 \text{ cm}^3/\text{s}$  and a gas flow rate of  $1.7 \text{ cm}^3/\text{s}$ .

To the best of the author's knowledge, there is not yet any CFD simulation of the two-phase flow in the SEN describing this phenomenon. Hence, a CFD modelling of the two-phase flow in the nozzle would be highly welcome for a critical assessment of the measurements published in Timmel et al. (2015). Further measurement data might be provided in case of interest.

Downstream in the mould the vast majority of bubbles leaving the nozzle are carried by the discharging jet into the lower circulation roll where they remain for many recirculation periods. The bubbles exhibit a long residence time in the lower circulation roll of the mould flow. Larger bubbles develop owing to coalescence and rise sporadically towards the free surface as visible in Fig. 8.

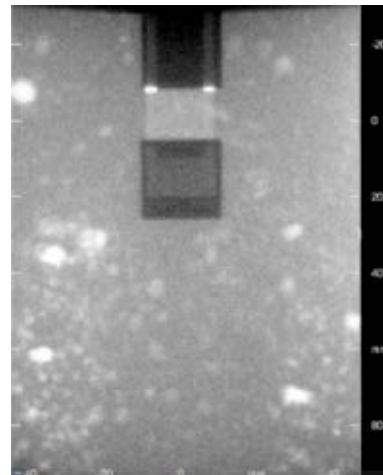


Figure 8: Snapshot showing the gas distribution in the mould at X-LIMMCAST with a liquid flow rate of  $140 \text{ cm}^3/\text{s}$  and a gas flow rate of  $0.7 \text{ cm}^3/\text{s}$ .

## FURTHER EXAMPLES OF LIQUID METAL MODEL EXPERIMENTS

Such model experiments are always useful as long as the real process under consideration is hardly accessible for experimental inspection. In the following we mention a few further examples.

The magnetic control of the down sprue flow in an industrial aluminum investment casting process was essentially based on GaInSn model experiments. They convincingly showed that the braking action of the external DC field can lead to a much more homogeneous distribution of the incoming melt over the cross-section of the duct, thus avoiding bubble or inclusion entrapment as they are typical for splashing melt fronts. For the particular casting part under consideration a significant reduction of the failure rate was obtained under industrial conditions. For more details we refer to Gerbeth et al. (2006).

Melt stirring by alternating magnetic fields is well-known for long. Standard stirring fields are the Rotating Magnetic Field (RMF), the Travelling Magnetic Field (TMF), or just the alternating magnetic field of a typical induction heater. Model experiments with the GaInSn melt allowed for verifying the calculated flow structures by direct velocity measurements. Interesting flow structures arise if the above stirring fields are superimposed. For instance, a certain combination of RMF and TMF gives rise to intense tornado-like flows as reported by Vogt et al. (2013). Note that these tornado-like flows by a suitable RMF-TMF combination have not yet been reproduced by CFD simulations in the turbulent parameter range.

Another focus of the experimental work is the investigation of the influence of electromagnetic fields on the process of solidification of metallic alloys. For that purpose an experimental setup has been made that enables for a simultaneous monitoring of the temporary position of the growth front, the temperature distribution and the flow pattern during solidification (see Fig. 9). This setup has been used for model experiments in Pb-Sn at temperatures of about 250°C and for investigations in Al-Si up to about 700°C.

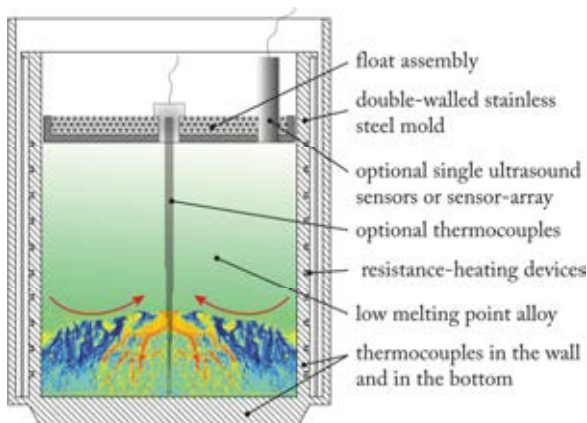


Figure 9: Schematic view of the setup for solidification experiments allowing for simultaneous observations of the front position, the temperature field and the velocity field.

The experiments provide an elaborate data base for the validation of numerical simulations. For that purpose, a network of cooperation exists with other numerical and experimental groups. A close collaboration with the University of Iowa focuses on fundamental aspects of the evolution of dendritic structures during the growth process and coarsening. The impact of fluid flow on the formation of segregation zones is investigated together with Oxford University (see Karagadde et al., 2014) and

Paris Mines Tech (see Saad et al., 2015). Furthermore, HZDR experimental data are also referred to on the webpage [www.solidification.org](http://www.solidification.org).

Electromagnetic stirring during solidification has been proved to be a striking method for achieving a purposeful alteration of the microstructure of casting ingots, such as grain refinement or the promotion of a transition from a columnar to an equiaxed dendritic growth (CET). However, the imposition of an RMF or a TMF also causes problems such as the occurrence of typical segregation pattern or a deflection of the upper free surface. A permanent radial inward (RMF and downward TMF) or outward (upward TMF) flow along the solidification front is responsible for the transport of solute to the axis or the wall of the ingot resulting in typical freckle segregation pattern filled with alloy of eutectic composition as shown for Al-Si experiments in Fig. 10a (freckles are highlighted by red framing). Our studies have been devoted to overcoming the handicaps of rotary stirring with the specific goal to generate a vigorous stirring in the bulk without considerable deformations of the free surface. So it was shown recently that the application of modulated AC magnetic fields offers considerable potential for optimizing the melt stirring. The secondary flow can be organized in such a way that periodic reversals of the flow direction occur adjacent to the solidification front, which has been proven as an important method to prevent flow-induced macrosegregation (see Eckert et al. (2007) and Willers et al. (2008)). Fig. 10b shows that the application of a pulsed RMF reduces the segregation effects significantly, which was demonstrated in Pb-Sn model experiments and afterwards also in Al-Si experiments.

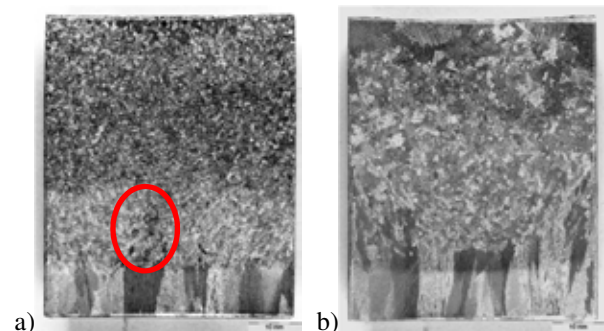


Figure 10: Comparison between a permanently applied RMF (left) and a modulated RMF (right) in Al-Si solidification: macrostructure of the longitudinal section.

## CONCLUSIONS

Liquid metal model experiments are a useful tool for various liquid metal processes, at least as long as the flow field and the related heat and mass transfer cannot be measured in the real, typically high-temperature processes. At much lower temperatures the model experiments allow today an almost complete measurement of the local flow field. This is of crucial importance for the validation of numerical simulations and for a better design or control of the corresponding liquid metal processes. The combination of numerical simulations with such model experiments often leads to a significantly improved insight into the processes.

## ACKNOWLEDGMENT

Financial support by the German Helmholtz Association in frame of the Helmholtz Alliance “Liquid Metal Technologies (LIMTECH)” is gratefully acknowledged.

## REFERENCES

- ECKERT, S. CRAMER, A. and GERBETH, G., (2007), “Velocity measurement techniques for liquid metal flows”, Molokov, S. et al. (Eds), *Magneto-hydrodynamics – Historical Evolution and Trends*, 275-294, Springer.
- ECKERT, S. et al., (2011), “Some recent developments in the field of measuring techniques and instrumentation for liquid metal flows”, *J. Nucl. Sci. & Technol.*, **48**, 490-498.
- WONDRAK, T. et al., (2014), “Measurement techniques for the flow in a model of a continuous caster”, *Proc. 8<sup>th</sup> ECCO*, Graz, Austria, June 23-26, 2014, 247-256.
- TAKEDA, Y., (1991), “Development of an ultrasound velocity profile monitor”, *Nucl. Eng. Des.*, **126**, 277-284.
- ECKERT, S. GERBETH, G. and MELNIKOV, V.I., (2003), “Velocity measurements at high temperatures by ultrasound Doppler velocimetry using an acoustic wave guide”, *Exp. Fluids*, **35**, 381-388.
- STEFANI, F., GUNDRUM, T. and GERBETH, G., (2004), “Contactless inductive flow tomography”, *Phys. Rev. E*, **70**, 056306.
- WONDRAK, T. et al., (2010), “Contactless inductive flow tomography for a model of continuous steel casting”, *Meas. Sci. Technol.*, **21**, 045402.
- WONDRAK, T. et al., (2011), “Combined electromagnetic tomography for determining two-phase flow characteristics in the submerged entry nozzle and in the mould of a continuous casting model”, *Metall. Mater. Trans. B*, **42**, 1201-1210.
- RATAJCZAK, M., WONDRAK, T. and STEFANI, F., (2016), “A gradiometric version of contactless inductive flow tomography: theory and first applications”, *Phil. Trans. Royal Soc. A*, **374**, 20150330.
- PLEVACHUK, Y. et al., (2010), “Thermophysical properties of liquid tin-bismuth alloys”, *Int. J. Mater. Res.*, **101**, 839-844.
- TIMMEL, K. et al., (2010), “Experimental modeling of the continuous casting process of steel using low melting point metal alloys – the LIMMCAST program”, *ISIJ Int.*, **50**, 1134-1141.
- TIMMEL, K. et al., (2015), “Visualization of liquid metal two-phase flows in a physical model of the continuous casting process of steel”, *Metall. Mater. Trans. B*, **46**, 700-710.
- TIMMEL, K. et al., (2011), “Experimental investigation of the flow in a continuous-casting mold under the influence of a transverse, direct current magnetic field”, *Metall. Mater. Trans. B*, **42**, 68-80.
- CHAUDHARY, R., THOMAS, B.G. and VANKA, S.P., (2012), “Effect of electromagnetic ruler braking (EMBr) on transient turbulent flow in continuous slab casting using large eddy simulations”, *Metall. Mater. Trans. B*, **43**, 532-553.
- MIAO, X., et al., (2012), “Effect of an electromagnetic brake on the turbulent melt flow in a continuous-casting mold”, *Metall. Mater. Trans. B*, **43**, 954-972.
- STEFANI, F. et al., (2006), “Experimental evidence for magnetorotational instability in a Taylor-Couette flow under the influence of a helical magnetic field”, *Phys. Rev. Lett.*, **97**, 184502.
- GERBETH, G. et al., (2006), “Use of magnetic fields in aluminum investment casting”, *Proc. EPM 2006*, Sendai, Japan, Oct. 23-27, 323-328.
- VOGT, T. et al., (2013), “Spin-up of a magnetically driven tornado-like vortex”, *J. Fluid Mech.*, **736**, 641-662.
- KARAGADDE, S. et al., (2014), “3-D microstructural model of freckle formation validated using in-situ experiments”, *Acta Mater.*, **79**, 168-180.
- SAAD, A. et al., (2015), “Simulation of channel segregation during directional solidification of In-75wt%Ga alloy: Qualitative comparison with in-situ observations”, *Metall. Mater. Trans. A*, **46**, 4886-4897.
- ECKERT, S. et al., (2007), “Efficient Melt Stirring Using Pulse Sequences of a Rotating Magnetic Field-Part I – Flow Field in a Liquid Metal Column”, *Metall. Mater. Trans. B*, **38**, 977-988.
- WILLERS, B. et al., (2008), “Efficient Melt Stirring Using Pulse Sequences of a Rotating Magnetic Field-Part II – Application to Solidification of Al-Si Alloys”, *Metall. Mater. Trans. B*, **39**, 304-316.